An Electrically-Detected Magnetic Resonance Study of the Atomic-Scale Effects of Fluorine on the Negative Bias Temperature Instability

J.T. Ryan[1] and P.M. Lenahan[2]
The Pennsylvania State University, University Park, PA 16802
Tel: 814-863-4630, Fax: 814-863-7967, Email: [1]jtr16@psu.edu, [2]pmlesm@engr.psu.edu

A.T. Krishnan[3] and S. Krishnan[4]
Texas Instruments, Dallas, TX 75243
Tel: 972-995-1183, Email: [3]anandtk@ti.com, [4]s-krishnan1@ti.com

J.P. Campbell
NIST, Gaithersburg, MD 20899
Tel: 301-975-8308, Email: jason.campbell@nist.gov

ABSTRACT

It has been shown that the negative bias temperature instability (NBTI) may be significantly suppressed through the incorporation of fluorine in the gate oxide. In this study, we use the electrically-detected magnetic resonance technique of spin dependent recombination and standard gated diode current measurements to investigate the atomic-scale processes involved in fluorine's suppression of NBTI. Our results indicate that fluorine effectively passivates Si/SiO_2 P_{b0} center defect precursors, but is much less effective at passivating Si/SiO_2 P_{b1} center defect precursors. Since these two defects have significantly different densities of states, our results maybe useful in modeling NBTI response in fluorinated oxide devices. Our results also help to provide a fundamental explanation for the observation that fluorination has a strong effect on NBTI in "pure" SiO_2 MOS devices, but is ineffective at reducing NBTI in nitrided oxide devices

INTRODUCTION

The negative bias temperature instability (NBTI) is one of the most important reliability problems in present day CMOS technology [1-4]. NBTI results in threshold voltage shifts and a degradation of saturation drive current when pMOSFETs are subjected to negative gate bias at moderately elevated temperatures [1, 5]. Aggressive gate oxide scaling and the incorporation of nitrogen in the gate stack has exacerbated NBTI in recent CMOS technology [1, 5].

The most widely accepted hypothesis of NBTI degradation, the reaction-diffusion model, involves the creation of Si/SiO_2 interface states (P_b centers) following a negative bias temperature stress (NBTS) [6-8]. During NBTS, it is believed that hydrogen is liberated from the Si/SiO_2 interface and diffuses into the SiO_2 which results in Si/SiO_2 interface states [6-8]. (The precise details of this process are still widely debated [2].) Recent work suggests that NBTI may be somewhat suppressed by incorporating fluorine in the gate oxide [3, 4]. These observations are consistent with earlier suggestions that fluorine may passivate Si/SiO_2 dangling bond defects more effectively than hydrogen [9]. Although progress has recently been made in identifying the atomic-scale defects responsible for NBTI in conventional SiO_2 and SiO_xN_y based devices [10, 11], not much is known about the atomic-scale effects of fluorine on NBTI.

Electron spin resonance (ESR) is arguably the only technique with the analytical power and sensitivity to observe the atomic-scale defects responsible for MOS instability problems [12]. In earlier studies, the analytical power of ESR has been successfully utilized to study NBTI induced interface state generation in SiO_2 based large area MOS capacitor structures [11]. An extremely sensitive, electrically-detected ESR technique called spin dependent recombination (SDR) has the added advantage of being able probe atomic-scale defects in fully processed MOSFETs. (Conventional ESR measurements are limited by sample requirements which dictate large area capacitor structures.) Recent work by Campbell *et al*. has utilized SDR in studying NBTI induced defects in SiO_2 and SiO_xN_y MOSFETs [10]. In this study, we employ SDR measurements to directly observe the atomic-scale effects of fluorine on NBTI response. Additional gated diode current measurements [13] (DC-IV) demonstrate a correlation between the SDR results and device parameter degradation. Our goal in this study is to begin to develop an atomic-scale understanding of the role fluorine plays in NBTI with the hope that this understanding will be helpful in developing processing techniques to ameliorate NBTI.

EXPERIMENTAL

Our study compares the effects of NBTS on conventional pure SiO_2 devices and very similar fluorinated SiO_2 devices. Both types of devices are large area (~40,000 μm^2) pMOSFETs with identical gate oxide thickness (7.5 nm) and device geometry. Three differently processed sets of fluorinated devices where used.

SDR and DC-IV measurements were made before and after identical NBTS sequences (devices were subjected to a gate bias of -5.7 V at 140°C for 250,000 seconds). Following NBTS, all of the devices were subject to a temperature quench in which the stressing temperature is reduced to room

 978-1-4244-2195-4/08/$25.00 ©2008 IEEE

temperature over approximately 4 minutes while the gate bias stress is maintained. We have found this method to be fairly effective at "locking-in" the NBTI-induced damage, rendering it observable in the SDR/DC-IV measurements [14]. SDR measurements were made at room temperature on a custom-built X-band spectrometer based on a Resonance Instruments 8330 series microwave bridge and TE_{102} microwave cavity. The SDR measurements were calibrated using a strong pitch spin standard.

RESULTS AND DISCUSSION

Figure 1 illustrates representative pre- and post- NBTS DC-IV curves for the pure SiO_2 (Fig. 1a) and fluorinated SiO_2 (Fig. 1b) devices. The peak in the post-NBTS DC-IV curve, which scales with interface state density (D_{it}), is nearly an order of magnitude smaller in the fluorinated case (Fig. 1b). Following the analysis of Fitzgerald and Grove [13] and assuming a mean capture cross section of $\sigma = 2 \times 10^{-16} cm^2$, D_{it} values were extracted. For pure SiO_2 (Fig. 1a), $D_{it} = 7 \times 10^9$ $cm^{-2}eV^{-1}$ for pre-NBTS and 5×10^{11} $cm^{-2}eV^{-1}$ for post-NBTS. For the representative fluorinated SiO_2 sample (Fig. 1b), $D_{it} = 8 \times 10^9$ $cm^{-2}eV^{-1}$ for pre-NBTS and 9×10^{10} $cm^{-2}eV^{-1}$ for post-NBTS. The reduction in post-NBTS D_{it} of Fig. 1b (compared to the nearly identical pure SiO_2 sample) was observed in all three sets of fluorinated SiO_2 devices in our study. This is consistent with other reports which indicating less NBTI damage in fluorinated SiO_2 devices [3, 4].

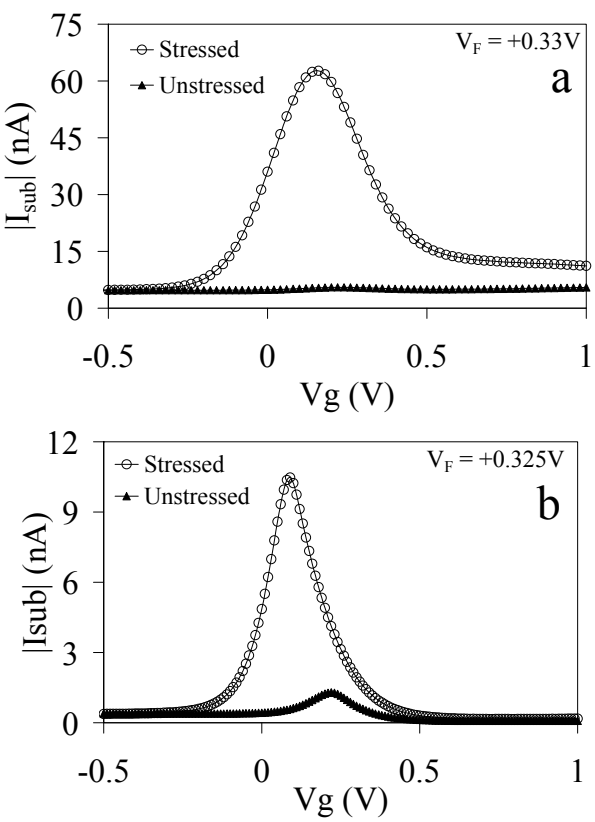

Figure 1: Representative pre- and post- NBTS DC-IV curves for pure SiO_2 (a) and fluorinated SiO_2 (b) devices. The smaller post-NBTS D_{it} for the fluorinated devices was consistently observed in our study.

Figure 2 compares SDR traces of the two post-NBTS devices utilized in Fig. 1. Pre-NBTS defect spectra were below the detection limit of the spectrometer. Note that in this figure, the spectrometer gain for the pure SiO_2 trace (Fig. 2a) is much lower than the fluorinated SiO_2 trace (Fig. 2b). Fig. 2a exhibits two somewhat overlapping signals with g values of 2.0057 and 2.0031 which are respectively due to Si/SiO_2 P_{b0} and P_{b1} centers [12, 15]. (The g is defined as $g = h\nu/\beta H$, where h is Planck's constant, ν is the microwave frequency, β is the Bohr magneton, and H is the magnetic field at resonance. The g depends on the defect's structure and orientation with respect to the applied magnetic field; it is essentially a second rank tensor.) Note that Fig. 2a is representative of NBTI SDR results on many essentially pure SiO_2 pMOSFETs, as reported earlier [10, 16]. The Fig. 2b trace exhibits a significantly different and much weaker single line spectrum with a g of 2.0026 which is consistent with a P_{b1} center.

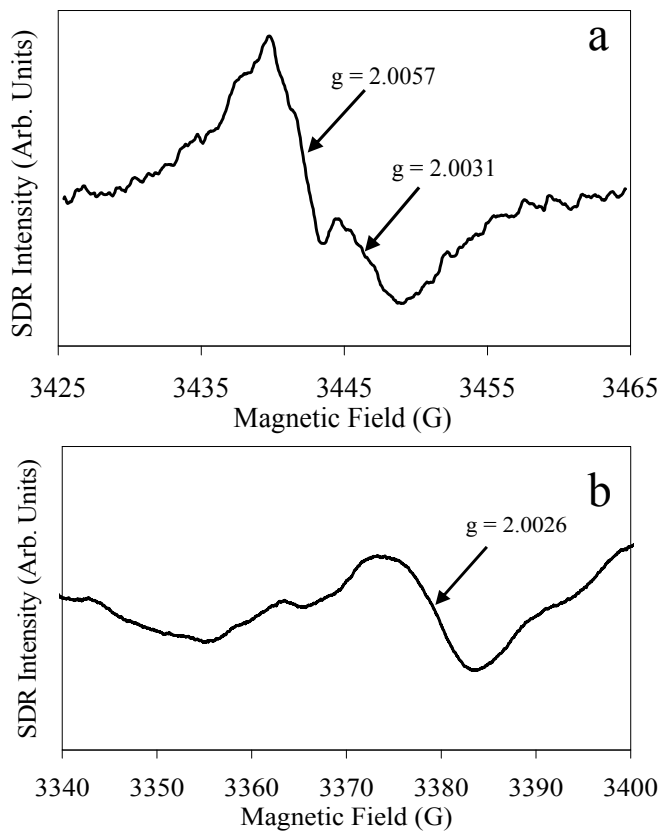

Figure 2: Post-NBTS stressing SDR traces for the pure SiO_2 (a) and fluorinated SiO_2 (b) devices of Fig. 1. Spectrometer settings are different; the gain is much higher and the sweep width greater to compensate for the much weaker and somewhat broader fluorinated oxide signal (b).

Although the devices of Fig. 2 are very similar structurally and were stressed in identical ways, their NBTI response is vastly different. For the case of the fluorinated device, there is no indication of P_{b0} center generation during NBTS. This observation suggests that the incorporation of fluorine is selectively passivating P_{b0} center precursors, or is more effective at passivating the P_{b0} center precursors.

Figure 3 illustrates (weak) post-NBTS SDR traces for the remaining two types of somewhat differently processed fluorinated SiO_2 devices. Again, pre-NBTS defect spectra are below the detection limit of the spectrometer. Note the same qualitative pattern; a weak SDR signal at $g \approx 2.003$ (which is consistent with P_{b1} center generation) and an absence of spectra expected for P_{b0} defects. DC-IV measurements (not shown) for the device from Fig. 3a indicate pre-NBTS $D_{it} = 2 \times 10^{10}$ $cm^{-2}eV^{-1}$ and post-NBTS $D_{it} = 1 \times 10^{11}$ $cm^{-2}eV^{-1}$. For the device from Fig. 3b, pre-NBTS $D_{it} = 1 \times 10^{10}$ $cm^{-2}eV^{-1}$ and post-NBTS $D_{it} = 1 \times 10^{11}$ $cm^{-2}eV^{-1}$.

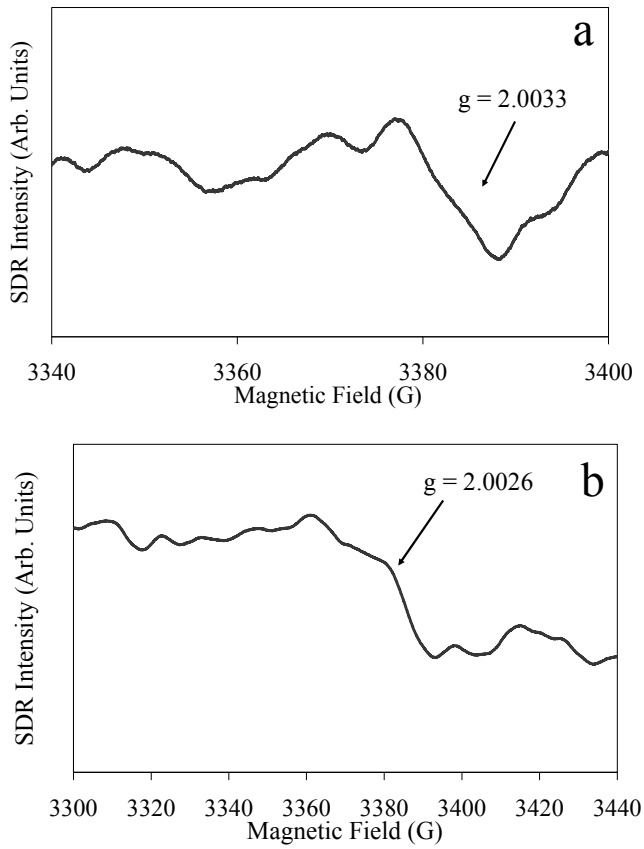

Figure 3: Post-NBTS SDR traces of the remaining two types of differently processed fluorinated devices. The qualitative pattern is identical; a weak P_{b1} signal and an absence of P_{b0} signal. Note the increased line width of the signal in trace b.

As mentioned previously, these results quite strongly suggest that fluorine incorporation can effectively passivate P_{b0} center precursors, but less effectively passivate P_{b1} center precursors. This would help to explain the diminished interface state generation observed in other recent reports of NBTI stressed fluorinated devices [3, 4]. Note the increased breadth of the signal in Fig. 3b. This may indicate the presence of nearby fluorine nuclei [17].

P_{b0} and P_{b1} defects are both silicon dangling bond defects in which the central silicon atom is back-bonded to three other silicon atoms precisely at the Si/SiO_2 boundary [12, 15]. A schematic illustration of P_{b0} and P_{b1} center structure is provided in Fig. 4. They are the two variants of defect centers that dominate interface trapping at (100) Si/SiO_2 boundaries and are responsible for a wide range of MOS instability and performance issues [12]. These defects are apparently responsible for the commonly observed increase in D_{it} following NBTI stressing of pure SiO_2 devices [10, 11].

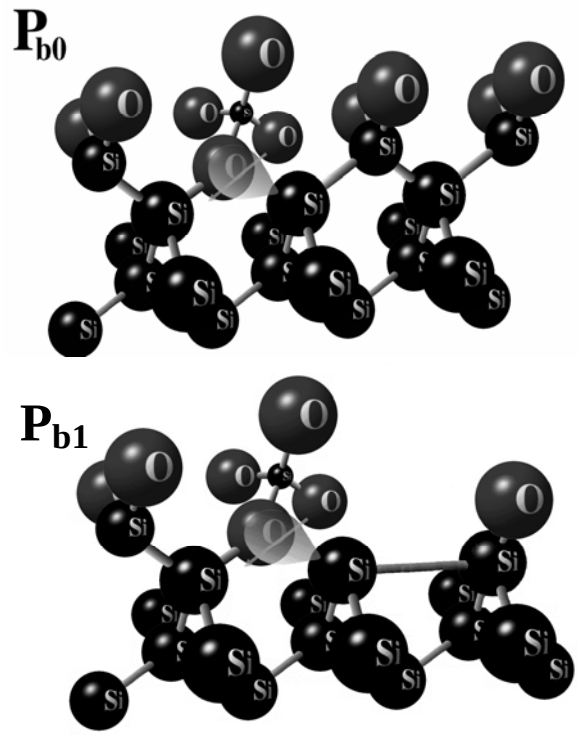

Figure 4: Schematic illustrations of P_{b0} (top) and P_{b1} (bottom) structure.

The main differences between the two defects are in the dangling bond axis of symmetry and their electronic density of states (illustrated in figure 5). The P_{b0} dangling bond orbital points along <111> directions, while the P_{b1} dangling bond orbital points along <211> directions [15, 18, 19]. P_{b0} centers have a broadly peaked density of states centered about midgap with an electron correlation energy of about 0.7eV [20, 21]. The P_{b1} levels are much more narrowly distributed, with a density of states skewed towards the lower half of the silicon band gap [21].

Since these defects have significantly different densities of states, our results maybe useful in modeling NBTI response in fluorinated oxide devices. The narrower P_{b1} density of states distribution will likely result in a larger shift in threshold voltage in proportion to the total number of P_{b1} states. That is, a higher percentage of P_{b1} centers will likely be positively charged when the pMOS transistor is on. This larger effect per defect is of course compensated by the smaller total number of P_{b1} centers. The result also helps explain why fluorine reduces NBTI damage in pure SiO_2 devices, but not in some nitrided devices; in nitrided devices, NBTI is not dominated by P_b centers [10].

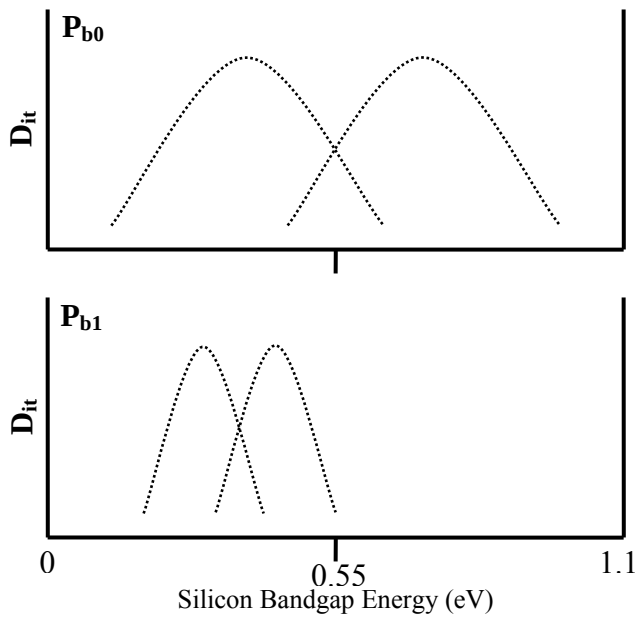

Figure 5: Schematic illustration of P_{b0} (top) and P_{b1} (bottom) density of states distribution.

CONCLUSIONS

In summary, our results demonstrate that the incorporation of fluorine can diminish NBTI degradation in agreement with other recent work [3, 4]. Our results strongly indicate that fluorine incorporation in the SiO_2 can effectively passivate P_{b0} center precursors, but is less effective at passivating P_{b1} center precursors. As a result, P_{b1} centers dominate the resulting NBTI induced defect spectra. Work at Penn State was supported by Texas Instruments through Semiconductor Research Corporation custom funding.

REFERENCES

[1] M. A. Alam and S. Mahapatra, "A Comprehensive Model of PMOS NBTI Degradation", *Microelectron. Reliab.*, **45**, pp. 71-81 (2005)

[2] S. Chakravarthi *et al.*, "A Comprehensive Framework for Predictive Modeling of Negative Bias Temperature Instability," *Proc. IEEE Int. Reliab. Phys. Symp.*, pp. 273-282 (2004)

[3] T. B. Hook *et al.*, "The Effects of Fluorine on Parametrics and Reliability in a 0.18um 3.5/6.8 nm Dual Gate Oxide CMOS Technology", *IEEE Trans. Elec. Dev.*, **48**, pp. 1346-1353 (2001)

[4] C. H. Liu *et al.*, "Mechanism and Process Dependence of Negative Bias Temperature Instability (NBTI) for pMOSFETs with Ultrathin Gate Dielectrics", *IEEE IEDM Tech. Dig.*, pp. 509-512 (2002)

[5] D. K. Schroder and J.A. Babcock, "Negative Bias Temperature Instability: Road to Cross in Deep Submicron Silicon Semiconductor Manufacturing", *J. Appl. Phys.*,, **94**, pp. 1-18 (2003)

[6] K. O. Jeppson and C. M. Svensson, "Negative Bias Stress of MOS Devices at High Electric-Fields and Degradation of MNOS Devices", *J. Appl. Phys.*, **48**, pp. 2004-2014 (1977)

[7] C. E. Blat *et al.*, "Mechanism of Negative-Bias-Temperature Instability", *J. Appl. Phys.*, **69**, pp. 1712-1720 (1991)

[8] S. Ogawa *et al.*, "Interface-Trap Generation at Ultrathin SiO_2 (4-6 nm)-Si Interfaces During Negative-Bias Temperature Aging", *J. Appl. Phys.*, **77**, pp. 1137-1148 (1995)

[9] P. J. Wright and K. C. Saraswat, "The Effect of Fluorine in Silicon Dioxide Gate Dielectrics", *IEEE Trans. Elec. Dev.*, **36**, pp. 879-889 (1989)

[10] J. P. Campbell *et al.*, "Atomic-Scale Defects Involved in the Negative-Bias Temperature Instability", *IEEE Trans. Dev. Mater. Reliab.*, **7**, pp. 540-557 (2007)

[11] S. Fujieda *et al.*, "Interface Defects Responsible for Negative-Bias Temperature Instability in Plasma-Nitrided SiON/Si(100) Systems", *Appl. Phys. Lett.*, **82**, pp. 3677-3679 (2003)

[12] P. M. Lenahan and J.F. Conley, "What Can Electron Paramagnetic Resonance Tell Us About the Si/SiO_2 System?" *J. of Vac. Sci. Tech. B*, **16**, pp. 2134-2153 (1998)

[13] D. J. Fitzgerald and A. S. Grove, "Surface Recombination in Semiconductors", *Surf. Sci.*, **9**, pp. 347-369 (1968)

[14] J. P. Campbell *et al.*, "Observations of NBTI-Induced Atomic-Scale Defects", *IEEE Trans. Dev. Mater. Reliab.*, **6**, pp. 117-122 (2006)

[15] K. L. Brower, "Structural Features at the $Si-SiO_2$ Interface", *Z. Phys. Chem.*, **151**, pp. 177-189 (1987)

[16] J. P. Campbell *et al.*, "Direct Observation of the Structure of Defect Centers Involved in the Negative Bias Temperature Instability", *Appl. Phys. Lett.*, **87**, pp. 204106 (2005)

[17] J. H. Weil, J. R. Bolton, and J. E. Wertz, "Electron Paramagnetic Resonance", Wiley, New York (1994)

[18] J. W. Gabrys *et al.*, "High-Resolution Spin-Dependent Recombination Study of Hot-Carrier Damage in Short-Channel MOSFETs - Si^{29} Hyperfine Spectra", *Microelectron. Engr.*, **22**, pp. 273-276 (1993)

[19] T. D. Mishima and P. M. Lenahan, "A Spin-Dependent Recombination Study of Radiation-Induced P_{b1} Centers at the (001) Si/SiO_2 Interface", *IEEE Trans. Nucl. Sci.*, **47**, pp. 2249-2255 (2000)

[20] E. H. Poindexter *et al.*, "Electronic Traps and P_b Centers at the Si/SiO_2 Interface: Band-Gap Energy Distribution", *J. Appl. Phys.*, **56**, pp. 2844-2849 (1984)

[21] J. P. Campbell and P. M. Lenahan, "Density of States of P_{b1} Si/SiO_2 Interface Trap Centers", *Appl. Phys. Lett.*, **80**, pp. 1945-1947 (2002)